

Temperature compensation method for resonant microsensors based on a controlled stiffness modulation

Jae Hyeong Seo, Kemal Safak Demirci, Albert Byun, Stuart Truax, and Oliver Brand

Citation: *J. Appl. Phys.* **104**, 014911 (2008); doi: 10.1063/1.2952050

View online: <http://dx.doi.org/10.1063/1.2952050>

View Table of Contents: <http://jap.aip.org/resource/1/JAPIAU/v104/i1>

Published by the [American Institute of Physics](#).

Related Articles

Low-frequency noise in gallium nitride nanowire mechanical resonators

Appl. Phys. Lett. **101**, 233115 (2012)

Focused ion beam milling and deposition techniques in validation of mass change value and position determination method for micro and nanomechanical sensors

J. Appl. Phys. **112**, 114509 (2012)

Nanoscale spatial resolution probes for scanning thermal microscopy of solid state materials

J. Appl. Phys. **112**, 114317 (2012)

Size-variable droplet actuation by interdigitated electrowetting electrode

Appl. Phys. Lett. **101**, 234102 (2012)

Influence of a superficial field of residual stress on the propagation of surface waves—Applied to the estimation of the depth of the superficial stressed zone

Appl. Phys. Lett. **101**, 234104 (2012)

Additional information on J. Appl. Phys.

Journal Homepage: <http://jap.aip.org/>

Journal Information: http://jap.aip.org/about/about_the_journal

Top downloads: http://jap.aip.org/features/most_downloaded

Information for Authors: <http://jap.aip.org/authors>

ADVERTISEMENT



AIP Advances

Now Indexed in Thomson Reuters Databases

Explore AIP's open access journal:

- Rapid publication
- Article-level metrics
- Post-publication rating and commenting

Temperature compensation method for resonant microsensors based on a controlled stiffness modulation

Jae Hyeong Seo, Kemal Safak Demirci, Albert Byun, Stuart Truax, and Oliver Brand^{a)}

School of Electrical and Computer Engineering, Georgia Institute of Technology, Atlanta, Georgia 30332-0250 USA

(Received 7 December 2007; accepted 1 May 2008; published online 9 July 2008)

A strategy to compensate for frequency drifts caused by temperature changes in resonant microstructures is presented. The proposed compensation method is based on a controlled stiffness modulation of the resonator by an additional feedback loop to extract the frequency changes caused by temperature changes. The feasibility of the suggested method is verified experimentally by compensating for temperature-induced frequency fluctuations of a micromachined resonator. The developed compensation scheme requires only one additional feedback loop and is applicable to any resonant microstructure featuring excitation and detection elements. © 2008 American Institute of Physics. [DOI: [10.1063/1.2952050](https://doi.org/10.1063/1.2952050)]

I. INTRODUCTION

The output signal of a microsensor is a mixture of the sensor's response to the measurand of interest and to internal/external disturbances caused by, e.g., environmental changes. Suppression and/or compensation of the sensor response to these interfering factors are generally indispensable in order to achieve a high sensor resolution.

In the case of mass-sensitive resonant microsensors,¹⁻⁴ the resonance frequency of a vibrating microstructure is influenced not only by mass but also by stiffness changes of the mechanical structure itself. Microresonators typically show high mass sensitivities inherited from their small mechanical dimensions, but they respond sensitively to environmental changes as well. Therefore, for a microresonator to be used as a mass-sensitive sensor, e.g., in chemical and biochemical sensing applications, the mass sensitivity should be maximized, while the frequency drift by environmental effects and structure aging must be kept as small as possible. However, as most mass-sensitive sensors require to be exposed to the surrounding environment to allow interaction with, e.g., target analytes, resonance frequency changes caused by a changing environment are difficult to avoid.

Temperature-induced changes in the elastic modulus of the resonator materials and/or dimensional changes of the resonator structure itself are the most well known causes of a resonance frequency drift of a microresonator.^{5,6} Humidity,^{7,8} surface oxidation with time,⁹ ionic reactions on the resonator surface,¹⁰ and stress induced by the packaging⁶ under varying temperature and/or humidity are other environmental effects that can alter the mechanical stiffness of a resonator and, therefore, its mechanical resonance frequency. Finally, aging caused by mechanical fatigue from a long-term operation of the resonator contributes to the mechanical stiffness change as well.^{11,12} Arguably, the temperature is the most critical environmental factor limiting the resolution of mass-

sensitive resonant sensors. Therefore, compensating for the frequency drift caused by a temperature change is indispensable to achieve high sensor resolution.

To overcome the above mentioned limitations of resonant sensors, several compensation schemes have been investigated and are briefly highlighted in the following.

A standard approach for temperature compensation is to place a temperature sensor close to the microresonator. Thus, temperature is measured by means of a temperature sensitive device and a premeasured dependence of the resonance frequency on the temperature is used for compensation.¹³ For accurate temperature compensation, not only a precise temperature measurement but also a reproducible relation between temperature and resonance frequency is required. However, thermal time constants, thermal gradients between resonator and temperature sensor, and temperature sensor instabilities can cause inaccurate temperature measurements, thus leading to insufficient temperature compensation. Furthermore, any hysteresis in the temperature coefficient of the resonance frequency (TCf) caused by dynamic temperature variations and structure aging limits the effectiveness of this approach.

A second widely used approach, particularly for chemical and biochemical sensors, utilizes an additional resonator as a reference element to compensate for the temperature-induced frequency drift of the resonator.¹⁴⁻¹⁷ Sensing and reference resonators, with and without sensitive layer coating, respectively, are operated under the same environmental conditions. The basic idea behind this approach is that any environmental change except a mass change by analyte absorption will cause the same frequency drift to both the sensing and the reference resonator. Therefore, the frequency change by the added mass can be extracted from the frequency difference between the reference and the sensing resonator. Besides temperature, other environmental factors, such as humidity, density, and viscosity changes of the surrounding fluid, can be compensated as well with this method.¹⁷ For a precise compensation, sensing and reference resonators must have same mechanical properties or must at

^{a)}Tel.: +1-404-894-9425. FAX: +1-404-894-4700. Electronic mail: oliver.brand@ece.gatech.edu.

least show the same relative responses to the changing environmental factors.¹³ However, every resonator, even if fabricated on the same chip/wafer, has slightly different mechanical properties and, thus, slightly different resonance frequencies. In addition, mechanical stress and dimensional changes caused by the swelling of the sensitive layer coating upon exposure to analyte and/or humidity might also affect the frequency difference.⁸ Finally, temperature differences between reference and sensing resonators might result from a chemical reaction in the sensitive layer or from thermal gradients between the resonators, thus impeding proper compensation.

To avoid the challenges associated with a separate element for temperature sensing, a method exploiting two resonance modes of a single resonator has been developed.^{18,19} By exciting the resonator at two different resonance modes with different TCF's and by monitoring frequency changes of each vibration mode, the temperature can be extracted and the temperature-induced frequency drift can be compensated for. This approach has several attractive advantages: As the resonator itself is used for temperature sensing, there is no need for an external temperature sensor, and errors caused by, e.g., thermal gradients between temperature sensor and resonator are avoided. In addition to temperature, other environmental factors are expected to be compensated for as well using multiple vibration modes. However, the excitation and detection elements of the resonator must be designed to sustain stable harmonic oscillation at multiple resonance modes, thus limiting its application to certain resonator structures. In Ref. 20, a similar principle is used to design a temperature sensor from two micro-resonators with tailored frequency-temperature characteristics. Combined with an array of microresonators, each of them having a slightly different center frequency, this concept ensures frequency stability of a silicon-based reference oscillator over a large temperature range.²⁰

In this paper, we introduce a new compensation technique suitable for microresonators operated in a closed loop. The method relies on the controlled modulation of the mechanical stiffness of the resonators using an additional feedback loop and can be used to compensate for temperature-induced frequency drift. The proposed method does not require additional transducer elements and can be applied to any resonators featuring excitation and detection elements.

II. PRINCIPLE OF TEMPERATURE COMPENSATION

For the application as a mass-sensitive sensor, the microresonator is generally incorporated in an amplifying feedback loop as the frequency-determining element. The force-deflection relation of a mechanical resonator, modeled as a simple harmonic oscillator consisting of mass, damper, and spring, can be described by

$$m\ddot{x} + b\dot{x} + kx = F_m, \quad (1)$$

where m , b , k , x , and F_m denote effective mass, damping coefficient, mechanical spring constant, deflection, and excitation force, respectively.

If the excitation force F_m is in phase with the vibration velocity using a feedback loop, i.e., $F_m \propto \dot{x}$, and if the damping force $b\dot{x}$ in Eq. (1) is completely compensated by the excitation force $F_m = b\dot{x}$, then the effective damping coefficient of the closed loop system is zero and a self-sustaining oscillation can be initiated. Under weak or practically zero damping, the resonance frequency of the resonator is determined by

$$f_0 = \frac{1}{2\pi} \sqrt{\frac{k}{m}}. \quad (2)$$

Based on the linear model for a microresonator in Eqs. (1) and (2), the principle of the proposed temperature compensation method is described in the following.

A. Stiffness modulation

The force generated by the feedback loop must have the same phase as the vibration velocity of the oscillating resonator to sustain a harmonic oscillation, as explained before. If an additional excitation force is generated by another feedback loop and if this force is in phase with the deflection x of the oscillating resonator, the effective spring constant of the microstructure can be modified. For example, if the additional force F_c is represented by $F_c = Cx$, then the system equation of Eq. (1) is modified as

$$\begin{aligned} m\ddot{x} + b\dot{x} + kx &= F_m + F_c, \\ m\ddot{x} + b\dot{x} + (k - C)x &= F_m, \end{aligned} \quad (3)$$

where C is the artificial spring constant generated by the additional spring force F_c .

Then the resonance frequency of the microresonator in the feedback loop is changed in response to the modulated effective stiffness as

$$f_0 = \frac{1}{2\pi} \sqrt{\frac{k - C}{m}}. \quad (4)$$

This concept has been utilized for resonant magnetic field sensors where the stiffness modifying force is generated either passively using a permanent magnet²¹ or actively using a Lorentz force induced by an ac current in the presence of a (static) magnetic field.²² The spring constant of the resonator is modified in response to the magnetic field, and thus the magnetic field can be detected by measuring the resonance frequency change of the resonator. In these cases, the amplitude of the magnetically induced force, which is proportional to the measurand (magnetic field), is detected even though it is read out via a frequency change.

On the other hand, if the additional force F_c in Eq. (3) is generated utilizing a signal of an amplifying feedback loop itself by proper electronic circuitry, the stiffness of the resonator can be controlled by adjusting the force F_c . This fact, the controlled stiffness modulation by an additional feedback loop, is exploited here to estimate the temperature-induced frequency drift of a microresonator.

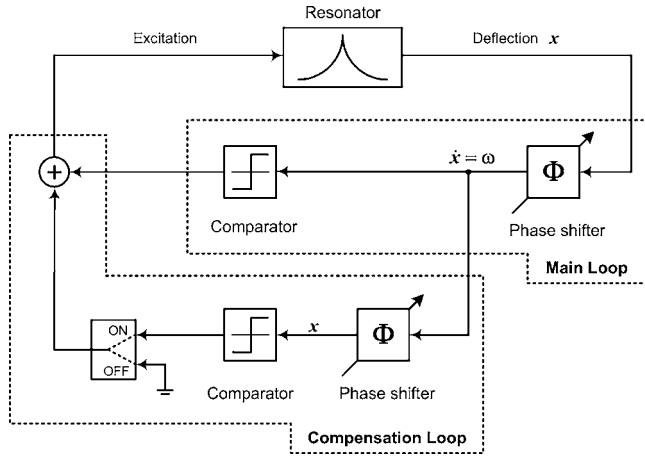


FIG. 3. Schematic diagram of feedback loop system to extract the relative Q -factor change of a resonator.

and detection can be done using a single element, and thus the product $\chi\gamma$ would be automatically independent of the environment.

C. Estimation of relative quality factor change

The direct estimation of the relative stiffness change of the resonator using the circuit shown in Fig. 1 has critical requirements for its application as mentioned above. Instead of a direct assessment of the relative stiffness change using the feedback system in Fig. 1, the relative quality factor change is considered in the following to compensate for the temperature influence on the resonance frequency.

The quality factor has been shown to be a good temperature sensor, and its use for compensating temperature-induced frequency drift of a resonator has been already reported.²³ In Ref. 23 the quality factor of the resonator was estimated by measuring the amplitude of the resonator output signal. However, a precise measurement of the resonator amplitude requires a carefully designed circuitry with a high signal to noise ratio, and an analog-to-digital converter is needed for compensating the temperature-induced frequency drift of the resonator.

In this section, a feedback system, which can extract the Q -factor of the resonator by measuring its resonance frequency, is introduced. Figure 3 shows the schematic diagram of the feedback loop for Q -factor estimation; compared to the compensation loop of Fig. 1, the linear amplifier is replaced by a comparator.

The motion of the resonator in this feedback loop can be described by

$$m\ddot{x} + b\dot{x} + kx = \psi_D \frac{\dot{x}}{|\dot{x}|} + \psi_C \frac{x}{|x|}, \tag{11}$$

$$\psi_D = \chi\gamma \frac{4M_d}{\pi}, \quad \psi_C = \chi\gamma \frac{4M_c}{\pi},$$

where M_d and M_c are the amplitudes of the square wave signals generated in the main loop and the compensation loop, respectively. Equation (11) can be rearranged to Eq. (12) to extract the vibration amplitude of the resonator,

$$m\ddot{x} + \left(b - \frac{\psi_D}{|\dot{x}|}\right)\dot{x} + \left(k - \frac{\psi_C}{|x|}\right)x = 0. \tag{12}$$

The magnitude of the steady state vibration velocity \dot{x} and the vibration amplitude x of the resonator embedded in the feedback circuit are obtained from Eq. (12) by forcing the effective damping force [second term in Eq. (12)] to zero,

$$|\dot{x}| = \frac{\psi_D}{b}, \quad |x| = \frac{\psi_D}{b\omega_0}. \tag{13}$$

Then, the differential equation of Eq. (12) can be expressed in terms of the Q -factor $Q_0 = kb^{-1}\omega_0^{-1}$ of the resonator using Eq. (13) as

$$m\ddot{x} + \left(k - \frac{\psi_C}{\psi_D}b\omega_0\right)x = 0 \Leftrightarrow m\ddot{x} + k\left(1 - \frac{\psi_C}{\psi_D} \frac{1}{Q_0}\right)x = 0. \tag{14}$$

Equation (14) reveals the interesting fact that the relative stiffness change induced by the feedback loop shown in Fig. 3 is directly related to the Q -factor of the resonator. Moreover, it does not depend on the absolute magnitude of the additional spring force but is proportional to the ratio of the two forces generated by the main loop and the compensation loop.

If the forces generated by the main and compensation loops are equal, i.e., $\Psi_D = \Psi_C$, Eq. (14) is simplified to Eq. (15), and the frequency ratios of the resonance frequencies with enabled and disabled compensation loops are determined by Eq. (16) at times t_1 and t_2 ,

$$m\ddot{x} + k\left(1 - \frac{1}{Q_0}\right)x = 0, \tag{15}$$

$$\left(\frac{\omega_{\text{on}}}{\omega_{\text{off}}}\right)^2 \Big|_{t=t_1} = \frac{Q_1 - 1}{Q_1} = \alpha, \quad \left(\frac{\omega_{\text{on}}}{\omega_{\text{off}}}\right)^2 \Big|_{t=t_2} = \frac{Q_2 - 1}{Q_2} = \beta. \tag{16}$$

Using Eq. (16), a direct measurement of the Q -factor is possible, and the relative Q -factor change with time can be derived the same way as in Eq. (8),

$$\frac{\Delta Q}{Q} = \frac{Q_2 - Q_1}{Q_1} = \frac{\alpha - \beta}{\beta - 1}. \tag{17}$$

As the excitation signals originating from both of the feedback loops are applied to the same excitation element, the temperature dependences of the excitation and detection elements do not cause errors in the measured Q -factor changes. This fact can be inferred from Eqs. (11) and (14). Therefore, a precise estimation of the relative Q -factor change is possible, irrespective of the chosen excitation and detection methods.

The quality factor is a complex parameter, which is related to all system constants in Eq. (1). From the linear model of a microresonator in Eq. (1), the relation of a relative Q -factor change to the system constants is derived as

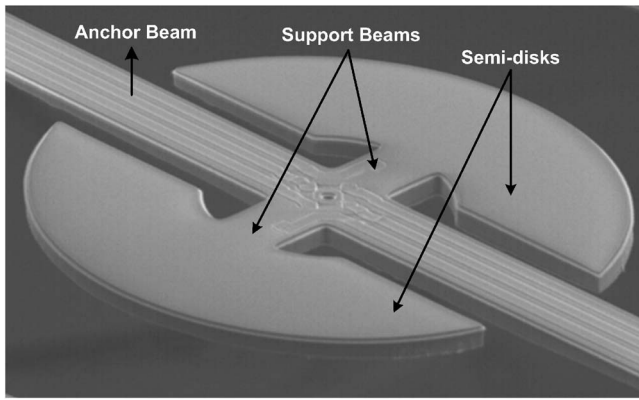


FIG. 4. SEM image of the rotational in-plane mode disk resonator.

$$Q = \frac{k}{b\omega_0} \rightarrow \frac{dQ}{Q} = \frac{dk}{k} - \frac{d\omega_0}{\omega_0} - \frac{db}{b}. \tag{18}$$

By combining the estimated relative Q -factor change (dQ/Q) and the measured relative frequency change ($d\omega_0/\omega_0$), the changes in the ratio of stiffness to the damping coefficient (k/b) of a microresonator are derived,

$$\frac{dQ}{Q} + \frac{d\omega_0}{\omega_0} = \frac{dk}{k} - \frac{db}{b}. \tag{19}$$

Once the relation of the relative change in k/b to the temperature is determined, the temperature-induced frequency drift of the microresonator can be compensated. Even though this approach requires a calibration step for temperature compensation, it has distinct advantages over the direct stiffness measurement using the feedback system in Fig. 1: (i) the precision of the extracted relative Q -factor change is not affected by temperature dependences of the excitation and detection elements of the resonator, (ii) the feedback system is more robust to noise in the output signal of the resonator, (iii) the amplitude of the square wave signal of the compensation loop is easier to be kept constant than the gain of a linear amplifier, (iv) besides the relative Q -factor change, a direct Q -factor estimation is possible.

Finally, if the relative damping coefficient change $\Delta b/b$ can be extracted from Eq. (13), e.g., by measuring the vibration amplitude of the resonator, the required calibration step can be potentially avoided and the relative change of all system constants of the resonator can be extracted.

III. EXPERIMENT

To verify the concept of the temperature compensation method introduced in this paper, the disk resonator shown in Fig. 4 has been used.²⁴ The silicon-based resonator features two semicircular disks, which are attached to a central silicon anchor beam through two support beams, and is designed to vibrate in a rotational in-plane resonance mode to minimize damping and, thus, achieve a high Q -factor. An asymmetric arrangement of two diffused heating resistors along the semi-disk's support beams, paired with proper excitation signals, generates the rotational torque by exploiting the difference in thermal expansion coefficients between aluminum and silicon. Silicon piezoresistors, arranged in a Wheatstone bridge around the center of rotation, are used for vibration detection. The excitation and detection elements are both implemented using boron-doped silicon resistors.

A direct estimation of the stiffness change using the schematic shown in Fig. 1 is challenging with the chosen disk resonators because of the temperature dependence of the resistors used as excitation and detection elements. Therefore, the temperature compensation method based on the estimation of the relative quality factor change using the circuit shown in Fig. 3 is mainly tested here. The relative quality factor change induced by a temperature variation is extracted according to Eq. (17), and, subsequently, the resulting temperature-induced frequency drift of the resonator is subtracted mathematically for compensation.

A. Feedback circuit and signal conditioning

The detailed schematic diagram of the implemented feedback circuitry is shown in Fig. 5. In the main loop, the piezoresistive output signal from the resonator is first amplified with an operational amplifier, and this signal is fed to a phase adjusting circuit (all-pass filter) to generate a signal

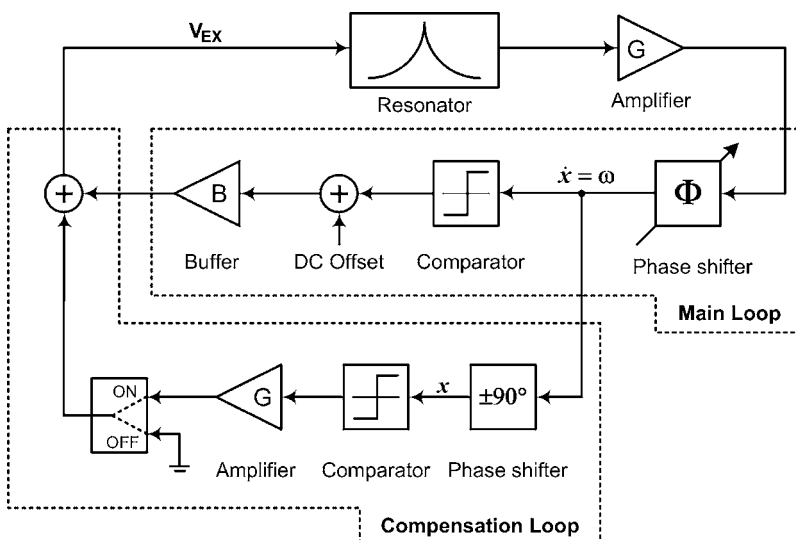


FIG. 5. Schematic diagram of the implemented feedback circuitry for temperature compensation.

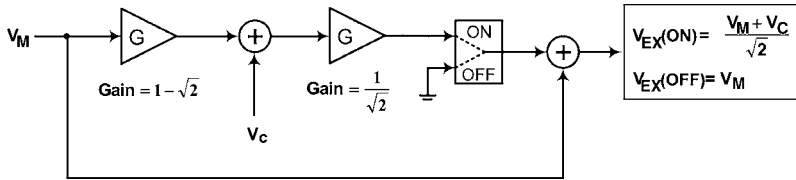


FIG. 6. Schematic of electronic circuitry to maintain constant static power dissipation in the resonator excitation elements.

that has the same phase as the vibration velocity of the resonator, which is 90° phase leading compared to the deflection signal. The phase tuning of each feedback loop must be done carefully to avoid/minimize errors in the estimated quality factor and, thus, to improve the accuracy of the temperature compensation.

It should be noted that the electrical output signal of the resonator is generally not in phase with the resonator deflection because of parasitic electrical coupling between excitation and detection signals. Therefore, the signal coming from the resonator is first phase tuned to match its phase to the vibration velocity by adjusting the phase shifter until the signal from the resonator reaches its maximum amplitude. The phase-tuned signal is then applied to a Schmitt-trigger circuit, which limits the signal amplitude. Thereafter, a dc bias voltage is added to the square wave signal to ensure that the thermally generated force has a component with the same frequency as the Schmitt trigger output signal. The resulting excitation signal is fed back to the resonator, sustaining the harmonic oscillation at the mechanical resonance frequency.

The phase shifter output signal of the main loop is connected to the compensation loop, which consists of a phase shifter, a Schmitt trigger, an adder, and a switch. The phase shifter generates a signal that is in phase with the resonator deflection, which is 90° phase delayed compared to the phase shifter output signal of the main loop. The Schmitt trigger limits the signal amplitude to a predefined value, and the switch is used to enable or disable the compensation loop.

The increased static power dissipation inside the resonator by the enabled compensation loop can cause a temperature elevation, resulting in a negative resonance frequency change due to the temperature-induced material softening. To keep the static power dissipation of the resonator constant regardless of the switch position, the excitation signal V_{ex} in Fig. 5 is adjusted using the operational amplifier circuit shown in Fig. 6. Thus, the excitation voltage V_{ex} depends on the switch position as

$$|V_M| = |V_C|,$$

$$V_{ex(on)} = \frac{V_M}{\sqrt{2}} + \frac{V_C}{\sqrt{2}}, \quad (20)$$

$$V_{ex(off)} = V_M,$$

where V_M , V_C , $V_{ex(on)}$ and $V_{ex(off)}$ are the signal amplitude from the main loop, the signal amplitude from the compensation loop, and the excitation signals when the switch is on and off, respectively.

B. Measurement setup and results

Experiments have been carried out with the test setup shown in Fig. 7. The closed loop system of Fig. 5 is implemented with a printed circuit board. The resonator is placed inside an ESPEC SH-241 environmental test chamber and connected through a cable to the printed circuit board located outside of the chamber to avoid temperature effects in the feedback circuitry. A LABVIEW program controls the switch position via a National Instrument data acquisition card and records the frequency of the resonator and the temperature of the chamber.

The compensation loop is enabled for 2 s every 52 s for all the experiments, and the resonance frequency of the resonator is recorded every second. The signal amplitudes of the main and compensation loops are both set to 400 mV by the respective voltage limiters. The test conditions and the properties of the resonator are summarized in Table I. The resonance frequency of the chosen resonator around 571 kHz is lowered by approximately 106 Hz at 45°C when the compensation loop is enabled, as shown in Fig. 8.

For an initial calibration, the disk resonator is operated under varying temperatures between 40 and 50°C . The frequency of the resonator is measured and the relative Q -factor change is extracted using the compensation loop. Figure 9 shows the measured relative frequency change and the extracted relative quality factor change of the resonator as a function of the temperature. The relative Q -factor and the relative frequency changes are calculated based on the values at 45°C . The estimated relative Q -factor changes and the resonance frequency exhibits a small hysteresis during thermal cycling, as can be noted in Figs. 9(a) and 9(b). Changes in thin film stresses during thermal cycling are well known causes of thermal hysteresis in micromachined sensors.^{25,26}

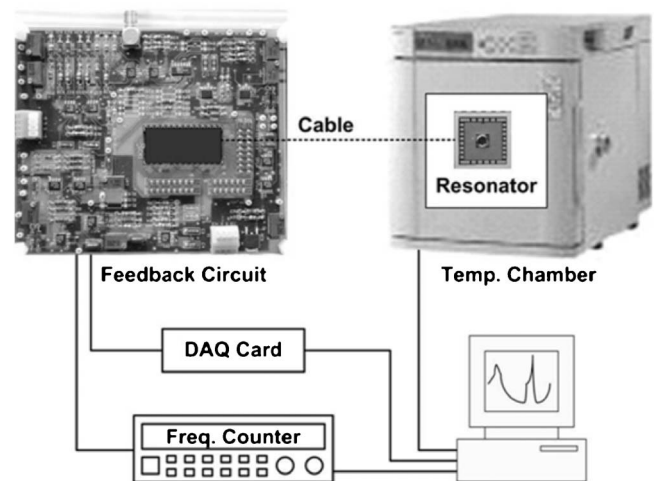


FIG. 7. Schematic diagram of the test setup.

TABLE I. Test conditions and properties of the disk resonator used for experiments.

Resonator radius	120 μm
Resonance frequency	571 kHz
Quality factor of the disk resonator in air	2800 at room temperature
Resistance of Wheatstone bridge	460 Ω
Resistance of heating resistors	890 Ω
Bias voltage for Wheatstone bridge	1.5 V _{dc}
dc offset voltage for excitation	0.75 V _{dc}
Amplitude of main-loop square wave	400 mV
Amplitude of compensation-loop square wave	400 mV

For fast calibration and simple temperature compensation without a look-up table, this thermal hysteresis is not considered during subsequent experiments. Instead, the relative Q -factor change and the relative frequency change are assumed to be linearly proportional to each other. From the plot of Fig. 9(c), the relation $dQ/Q_0 = 106.5d\omega/\omega_0$ is obtained using a least squares curve fit method, and the resulting proportionality factor is used to compensate for the temperature-induced resonance frequency change of the chosen resonator.

Following the initial calibration step, the resonator is operated over a wider temperature range to check the feasibility of the proposed compensation method. Figure 10 highlights the test results when the resonator is subjected to a temperature variation between 30 and 60 °C [see Fig. 10(a)]. The relative Q -factor change is extracted from Eq. (17) using the Q -factor at 45 °C as a base value. The extracted Q -factor change [see Fig. 10(b)] follows the temperature change. Figure 10(c) is the plot of the extracted Q -factor change as a function of temperature, again showing a thermal hysteresis behavior during thermal cycling as mentioned before. The temperature-compensated resonance frequency change is plotted in Fig. 11 along with the measured uncompensated frequency (dashed line). The frequency fluctuation is reduced to less than 15 Hz after compensation, showing that temperature-induced frequency changes can be effectively

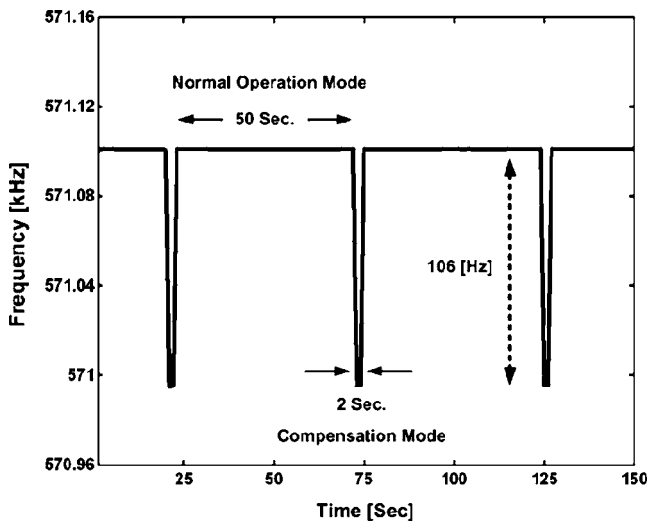


FIG. 8. Resonance frequency of disk resonator with and without compensation loop.

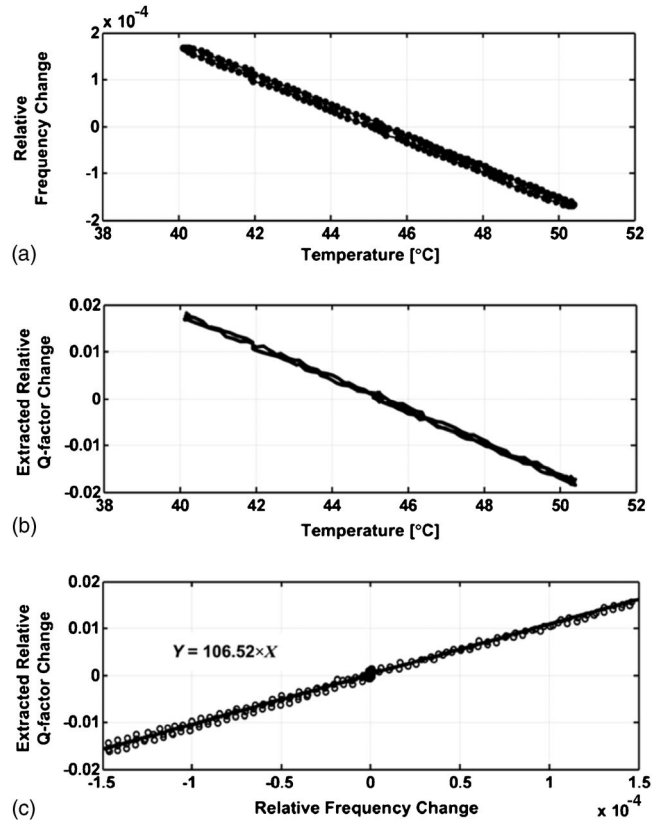


FIG. 9. Plot of (a) relative frequency change and (b) extracted relative Q -factor change as a function of temperature, and of (c) relative Q -factor change as a function of relative frequency change for temperatures in the range 40–50 °C. (c) Circles: extracted relative Q -factor changes; line: linear curve fit.

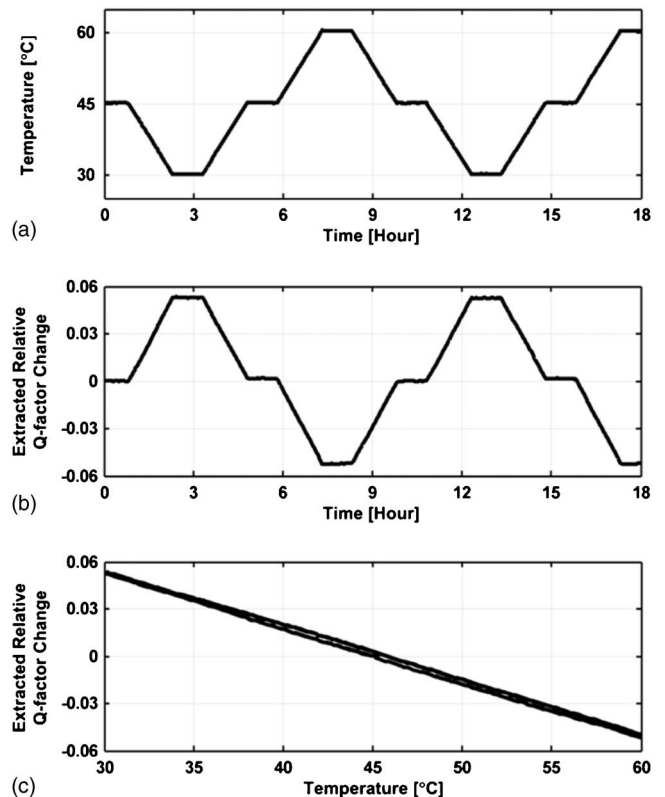


FIG. 10. (a) Ambient temperature and (b) extracted relative Q -factor change [from Eq. (17)] of a disk resonator subject to a predefined temperature profile; (c) extracted Q -factor change as a function of the ambient temperature.

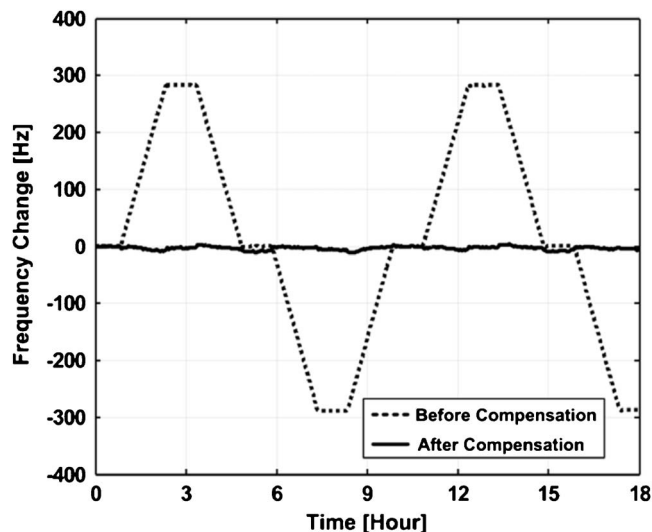


FIG. 11. Measured (dashed line) and compensated (solid line) resonance frequency changes of disk resonator subject to ambient temperature changes between 30 and 60 °C.

compensated for. The TCF of the resonator is reduced from -33.5 to -0.87 ppm/°C after compensating for the temperature-induced frequency drift.

To estimate the limit of the proposed method in compensating the temperature-induced frequency drift of a resonator, experiments were carried out under small temperature variations between 43 and 45 °C (see Fig. 12). In this case, the temperature-compensated resonance frequency shows around 3 Hz variations.

IV. CONCLUSION

A temperature compensation method for microresonators based on a controlled stiffness modulation by an additional electronic feedback loop is introduced in this paper. The temperature-induced frequency drift of the resonant microsensor can be compensated either directly by extracting the relative stiffness change of the resonator or indirectly by estimating the relative quality factor change.

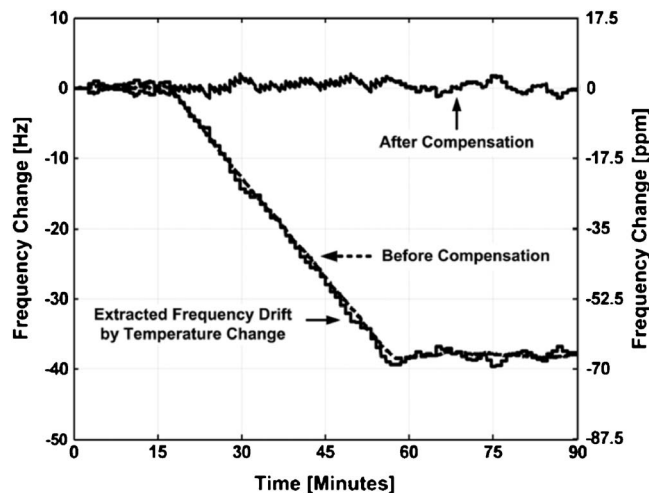


FIG. 12. Measured and compensated resonance frequency change of a resonator when subjected to a 2 °C temperature variation.

The indirect temperature compensation method, exploiting the temperature-induced quality factor change, is experimentally verified. The measurement results indicate that temperature-induced frequency changes even in the low ppm range can be compensated with this method. Particular advantages of the presented approach are as follows: (i) it requires only an additional feedback loop and, therefore, is applicable to any resonant sensors featuring excitation and detection elements without structural modifications, (ii) the temperature-induced frequency drift can be compensated without interrupting a sensor operation, (iii) the relative quality factor change of the resonator is extracted via a precise and simple frequency measurement, and (iv) the temperature dependences of the excitation and detection elements do not affect the precision of the proposed compensation method.

The direct temperature compensation method, based on the estimation of a relative stiffness change of a resonator, has not yet been experimentally verified. Applied to electrostatically or piezoelectrically excited/detected resonant sensors, it is, however, expected to work as well.

ACKNOWLEDGMENTS

This work has been supported in part by the National Science Foundation under Awards 0601467 and 0606981.

- ¹D. Lange, C. Hagleitner, A. Hierlemann, O. Brand, and H. Baltes, *Anal. Chem.* **74**, 3084 (2002).
- ²J. H. Seo, L. Betancor, K. S. Demirci, A. Byun, J. Spain, and O. Brand, in Proc. Solid-State Sensors, Actuators and Microsystems Conference (Transducers 2007), 2007, 1737–1740.
- ³N. V. Lavrik, M. J. Sepaniak, and P. G. Datskos, *Rev. Sci. Instrum.* **75**, 2229 (2004).
- ⁴R. Lucklum and P. Hauptmann, *Anal. Bioanal. Chem.* **384**, 667 (2006).
- ⁵F. L. Walls and J. J. Gagnepain, *IEEE Trans. Ultrason. Ferroelectr. Freq. Control* **39**, 241 (1992).
- ⁶R. Melamud, M. Hopcroft, C. Jha, K. Bongsang, S. Chandorkar, R. Candler, and T. W. Kenny, in Proc. Solid-State Sensors, Actuators and Microsystems Conference (Transducers 2005), 2005, pp. 392–395.
- ⁷A. Nakladal, K. Sager, and G. Gerlach, *Measurement* **16**, 21 (1995).
- ⁸T. Thundat, G. Y. Chen, R. J. Warmack, D. P. Allison, and E. A. Wachter, *Anal. Chem.* **67**, 519 (1995).
- ⁹J.-H. Jeong, S.-H. Chung, S.-H. Lee, and D. Kwon, *J. Microelectromech. Syst.* **12**, 524 (2003).
- ¹⁰T. Thundat, R. J. Warmack, G. Y. Chen, and D. P. Allison, *Appl. Phys. Lett.* **64**, 2894 (1994).
- ¹¹M. Koskenvuori, T. Mattila, A. Haara, J. Kiihamaki, I. Tittonen, A. Oja, and H. Seppa, *Sens. Actuators A115*, 23 (2004).
- ¹²R. L. Filler and J. R. Vig, *IEEE Trans. Ultrason. Ferroelectr. Freq. Control* **40**, 387 (1993).
- ¹³B. Roith, A. Gollwitzer, A. Lerner, and G. Fischerauer, in Proc. IEEE International Frequency Control Symposium and Exposition, 2006, pp. 827–830.
- ¹⁴T. W. Schneider, G. C. Frye-Mason, S. J. Martin, J. J. Spates, T. V. Bohuszewicz, G. C. Osbourn, and J. W. Bartholomew, *Proc. SPIE* **3539**, 85 (1998).
- ¹⁵J. H. Smith and S. D. Senturia, in Proc. Solid-State Sensors, Actuators and Microsystems Conference (Transducers 1995), 1995, pp. 724–727.
- ¹⁶T. Ono, D. F. Wang, and M. Esashi, in Proceedings of the IEEE Sensors Conference 2003, pp. 825–829.
- ¹⁷M. G. Schweyer, J. C. Andle, D. J. McAllister, and J. F. Vetelino, *Sens. Actuators B35*, 170 (1996).
- ¹⁸J. Veris, *Sens. Actuators, A* **57**, 179 (1996).
- ¹⁹J. R. Vig, *IEEE Sens. J.* **1**, 62 (2001).
- ²⁰E. P. Quevy and R. T. Howe, in Proceedings of the IEEE Radio Frequency

- Integrated Circuits (RFIC) Symposium, 2005, pp. 113–116.
- ²¹C. Seungkeun, K. Seong-Hyok, Y. Yong-Kyu, and M. G. Allen, [IEEE Trans. Magn.](#) **42**, 3506 (2006).
- ²²R. Sunier, T. Vancura, Y. Li, K.-U. Kirstein, H. Baltes, and O. Brand, [J. Microelectromech. Syst.](#) **15**, 1098 (2006).
- ²³M. A. Hopcroft, M. Agarwal, K. K. Park, B. Kim, C. M. Jha, R. N. Candler, G. Yama, B. Murmann, and T. W. Kenny, in Proceedings of the IEEE Conference on Microelectromechanical Systems, 2006, pp. 222–225.
- ²⁴J. H. Seo and O. Brand, [J. Microelectromech. Syst.](#) **17**, 483 (2008).
- ²⁵J. Thurn and R. F. Cook, [J. Appl. Phys.](#) **91**, 1988 (2002).
- ²⁶J. A. Chiou and S. Chen, [J. Microelectromech. Syst.](#) **14**, 782 (2005).